

<https://helda.helsinki.fi>

Restriction of plant roots in boreal forest organic soils affects the microbial community but does not change the dominance from ectomycorrhizal to saprotrophic fungi

Sietio, Outi-Maaria

2019-09

Sietio , O-M , Santalahti , M , Putkinen , A , Adamczyk , S , Sun , H & Heinonsalo , J 2019 , ' Restriction of plant roots in boreal forest organic soils affects the microbial community but does not change the dominance from ectomycorrhizal to saprotrophic fungi ' , FEMS Microbiology Ecology , vol. 95 , no. 9 , 133 . <https://doi.org/10.1093/femsec/fiz133>

<http://hdl.handle.net/10138/319702>
<https://doi.org/10.1093/femsec/fiz133>

Downloaded from Helda, University of Helsinki institutional repository.

This is an electronic reprint of the original article.

This reprint may differ from the original in pagination and typographic detail.

Please cite the original version.

1 **Restriction of plant roots in boreal forest organic soils affects the microbial community but does**
2 **not change the dominance from ectomycorrhizal to saprotrophic fungi**

3 Outi-Maaria Sietiö^{1,2}, Minna Santalahti^{1,2,3}, Anuliina Putkinen^{2,3}, Sylwia Adamczyk⁴, Hui Sun⁵, Jussi
4 Heinonsalo^{1,2,6}

5 ¹Department of Microbiology, University of Helsinki, Finland

6 ²Institute for Atmospheric and Earth System Research/Forest Sciences, Faculty of Agriculture and
7 Forestry, University of Helsinki, Finland

8 ³Department of Agricultural Sciences, University of Helsinki, Finland

9 ⁴Natural Resources Institute Finland, Finland

10 ⁵Collaborative Innovation Center of Sustainable Forestry in Southern China, College of Forestry,
11 Nanjing Forestry University, Nanjing, China

12 ⁶Finnish Meteorological Institute FMI, Climate System Research, Helsinki, Finland

13

14 Author for correspondence:

15 *Outi-Maaria Sietiö*

16 *Viikinkaari 9, Biocenter 1, 00790 Helsinki, Finland*

17 *Email: outi-maaria.sietio@helsinki.fi*

18 *tel. +358407613307*

19

20

21 **Abstract**

22 Boreal forest soils store significant amounts of carbon and are cohabited by saprotrophic and
23 ectomycorrhizal fungi (ECM). The “Gadgil effect” implies antagonistic interactions between
24 saprotrophic fungi and ECM. Plant photosynthates support the competitive fitness of the ECM, and
25 may also shape the soil bacterial communities. Many “Gadgil effect” experiments have focused on
26 litter layer (O_L) or have litter and root-fragments present, and thus possibly favor the saprotrophs. We
27 compared how the restriction of plant roots and exudates affect soil microbial community structures
28 in organic soil (mixed O_F and O_H). For this, we established a three-year field experiment with three
29 different mesh treatments affecting the penetration of plant roots and external fungal hyphae.
30 Exclusion of plant photosynthates induced modest changes in both fungal and bacterial community
31 structures, but not to potential functionality of the microbial community. The microbial community
32 was resilient towards rather short-term disturbances. Contrary to the “Gadgil effect”, mesh treatments
33 restricting the entrance of plant roots and external fungal hyphae did not favor saprotrophs that
34 originally inhabited the soil. Thus, we propose that different substrate preferences (fresh litter vs.
35 fermented or humified soil), rather than antagonism, maintain the spatial separation of saprotrophs
36 and mycorrhizal fungi in boreal forest soils.

37 **Keywords:** boreal forest soil, Gadgil effect, saprotrophs, ectomycorrhiza, microbial community,
38 functional gene profile

39 **Introduction**

40 The boreal forests form globally stable and large carbon (C) pools. In the organic layers of boreal
41 forest soils, carbon is stored in the form of complex polymers, including phenolic and humic
42 compounds (DeLuca and Boisvenue 2012). In boreal forest ecosystems the lack of easily available
43 nitrogen (N) in soils is considered to limit plant growth, since N is typically complexed with soil
44 minerals or organic compounds, which are unavailable to the plants (Schulten and Schnitzer 1998;
45 Näsholm, Kielland and Ganeteg 2009). To overcome the N limitation, plants form symbioses with
46 mycorrhizal fungi (Smith and Read 2008), which are efficient scavengers of N and other nutrients
47 from organic matter (Kohler *et al.* 2015; Shah *et al.* 2016).

48 The fungal and bacterial communities of boreal forest soils are interlinked and may either promote
49 each other's growth and functioning or suppress it through exudation of secondary metabolites (de
50 Boer *et al.* 2005). Mycorrhizal fungi can shape their associated bacterial community by carbon and
51 nutrient flows (Izumi and Finlay 2011) and different mycorrhizal fungi harbor different bacterial
52 populations (Skyring and Quadling 1969; Timonen and Sen 1998; Timonen *et al.* 1998). The fungal
53 and bacterial communities participate together in SOM decomposition and nutrient cycling in boreal
54 forest by producing various organic matter degrading enzymes and providing nutrients to each other
55 (de Boer *et al.* 2005). In nutrient limited ecosystems microbes may also compete for nutrients with
56 each other. Due to high diversity of microbes under different environmental conditions and niches,
57 the extent and nature of the dynamic interaction between fungi and bacteria in soil is still largely
58 unknown.

59 Although all fungal guilds can be found in all soil layers, the humus layers of the boreal forest
60 ecosystem are dominated by ectomycorrhizal (ECM) fungi whereas saprotrophs dominate the litter
61 layers (Lindahl *et al.* 2007; Santalahti *et al.* 2016). The growth and functioning of saprotrophic fungi
62 in humus layers might be restricted by the limited availability of easily utilizable N (Lindahl, Taylor

63 and Finlay 2002) or by the depletion of the labile C pool in SOM. The dominance of ECM over
64 saprotrophs in the boreal forest O_F and O_H layers is suggested to be maintained by the C flow from
65 the plants. The restriction of the plant-derived C to ECM can shift this dominance to saprotrophs and
66 other soil opportunists through a phenomenon called the Gadgil effect (Gadgil and Gadgil 1971, 1975;
67 Lindahl and Tunlid 2015; Averill and Hawkes 2016), and possibly change the decomposition rate.
68 However, contradictory results have been obtained and it is hypothesized that the role of ECM and
69 saprotrophic fungi and their interplay in litter and SOM decomposition is complex and affected by
70 various environmental conditions (Fernandez and Kennedy 2016). Since ECM fungi are supported
71 by the plant-C flow, they generally produce enzymes in order to acquire N, rather than C, from the
72 complex organic matter (Lindahl and Tunlid 2015; Bödeker *et al.* 2016). Scavenging for C from
73 humus, where C is stored in the form of complex polymers, is suggested to be unbeneficial for
74 saprotrophic fungi since the degradation process would require more energy than what could be
75 gained from the degraded substrate (Baldrian 2009). Consequently, saprotrophs dominate the
76 degradation of fresh plant litter.

77 Previous studies focusing on the effects of restricted plant carbon flow have been mainly
78 conducted in microcosms (Lindahl *et al.* 1999) or as short-term field experiments which also have
79 litter and root-fragments present (Gadgil and Gadgil 1971; Lindahl, de Boer and Finlay 2010;
80 Bödeker *et al.* 2016; Fernandez and Kennedy 2016). Therefore, in these experiments, there has been
81 plant biomass left in the soil to serve as an easy substrate for the saprotrophs. As proposed by Averill
82 & Hawkes (2016) and Fernandez & Kennedy (2016), in these studies the magnitude and presence of
83 the “Gadgil effect” might be mediated not only by the exclusion of the photosynthetic C flow but also
84 by the increase of labile-C input to soils due to the disturbance of the treatment. It is proposed that
85 the spatial separation of the ECM and saprotrophic guilds might also be due of different niche
86 preferences (Fernandez & Kennedy 2016), which is further supported by the difference in the
87 saprotrophic machineries between soil and litter saprotrophs and ECM fungi (Kohler *et al.* 2015).

88 To investigate the substrate dependence of the “Gadgil effect” we performed a field experiment in
89 a boreal forest over three growing seasons to determine how the manipulation of plant photosynthetic
90 C flow (1µm and 50 µm mesh treatments) affected the microbial communities and their potential
91 functionality in organic soil from O_F and O_H layers. We assumed that O_{F/H}-soil contains limited
92 amounts of labile-C, which is favored by saprotrophs. For this, we utilized a mesh bag approach
93 where bags with three different pore sizes 1000 µm (allow penetration of both fungal hyphae and fine
94 roots), 50 µm (allow fungal hyphae to penetrate but restrict tree-roots), and 1 µm (prevent the entrance
95 of both external fungal hyphae and all plant roots) were filled with sieved, non-sterile soil from O_F
96 and O_H layers. For studying the microbial community structures, we applied DNA-based MiSeq
97 sequencing combined with a GeoChip microarray and multivariate statistical analyses. We
98 hypothesized that the 1 µm mesh treatment restricting the entrance of plant photosynthates would: 1)
99 according to the “Gadgil effect” theory favor saprotrophs and that this change would be detectable as
100 increases in the relative abundance of saprotrophic taxa and in the potential functionality of these
101 treatments compared to the 50 µm and 1000 µm treatments, 2) change the overall fungal and bacterial
102 community compositions and their potential functionality compared to the 50 µm and 1000 µm
103 treatments. And 3) these changes in microbial communities will become more pronounced in time,
104 i.e. after 3rd growing season.

105

106 **Materials and methods**

107 **Experimental design**

108 The field experiment was conducted at Hyytiälä forestry field station (SMEAR II, University of
109 Helsinki) located in southern Finland (61°51' N, 24°17' E). The forest at Hyytiälä field station is
110 dominated by Scots pine (*Pinus sylvestris* L.) and the ground vegetation is dominated by shrubs and
111 mosses. For the experimental setup, soil from the organic layer (O_F and O_H) was collected from the

112 area surrounding Hyytiälä field station in autumn 2012. Prior to storing the collected organic soil at -
113 20°C, it was homogenized and sieved (4 mm mesh) but left otherwise untreated. This sieved and
114 homogenized non-sterile natural organic soil served later in the experiment as an initial fungal and
115 bacterial inoculum for the microbial community and repository of the initial soil fauna in the mesh
116 bags.

117 To manipulate the direct photosynthetic-C flows from the plants, mesh bags with three different
118 pore sizes (1000 µm, 50 µm and 1 µm (Fig. 1)) were filled with sieved and homogenized organic soil
119 from O_F and O_H layers corresponding to 14.2 g of dry weight. The different mesh sizes allowed
120 penetration of both fungal hyphae and fine roots (1000 µm), allowed fungal hyphae to penetrate but
121 restricted tree-roots (50 µm; the ericoid shrubs may have roots smaller in diameter than 50 µm), or
122 prevented the entrance of both external fungal hyphae and all plant roots (1 µm) (Wallander *et al.*
123 2001). In contrast to the traditional use of sterilized material (usually sand) in mesh bags, we used
124 unsterilized native organic soil for filling the mesh bags. Thus, the mesh bags contain also both living
125 and dead microbes acting as the initial inoculum inside the mesh bags later in the experiment.

126 The mesh bags were buried between organic and mineral soil horizons in May 2013 randomly at
127 three different sampling areas over 50 m apart from each other (described previously by Santalahti *et*
128 *al.* (2016)). All the selected experimental sites in Hyytiälä field station had similar above ground
129 vegetation and were visually uniform. One set of bags (n=15 for each mesh treatment, 3 sites with 5
130 replicates per site) were harvested yearly in late September after one, two and three growing seasons,
131 resulting in a total of 135 samples. The collected mesh bags were transported from the field to the
132 laboratory at +4 °C and divided into subsamples within the same working day as the harvest of the
133 mesh bags. The external roots colonizing the mesh bags were picked away from the soil samples and
134 their masses were recorded. Subsamples meant for molecular biology work were stored at -80 °C
135 before further analysis.

136 **Determination of mass loss, soil moisture, soil pH and fungal biomass from the individual mesh**
137 **treatments**

138 The soil moisture contents were determined from subsamples of each mesh bag by freeze drying
139 the soil for 3 days. The mass losses of the soil placed inside the different mesh bags were determined
140 by weighing the mesh bags at the time of the harvest and calculating the dry weight of the soil based
141 on the known soil moisture contents. The soil pH was measured from subsampled soil in a soil water
142 suspension of 1:2.5.

143 To assess the relative change in fungal biomass in each mesh treatment, ergosterol was extracted
144 as described in Frostegard & Bååth (1996) and measured using HPLC with an UV detector (HP
145 Agilent 1100). For the fungal biomass analysis, subsamples from each mesh size were pooled
146 separately within each year and within each sampling site, resulting in total three replicates from each
147 treatment in each sampling year (in total 27 samples). No initial time-point was analyzed for the
148 ergosterol.

149

150 **DNA extraction**

151 The total DNA was extracted from the freshly frozen soil samples (amount corresponding to 50
152 mg of dry weight) using the commercially available NucleoSpin Soil DNA extraction kit (Macherey-
153 Nagel GmbH & Co) with modifications described in Timonen et al. (2017). Extracted DNA was
154 further purified using a PowerClean Pro DNA Clean-Up kit (MoBio Laboratories) according to the
155 manufacturer's instructions. Concentrations of extracted dsDNA were measured fluorometrically
156 using a Qubit 2.0 Fluorometer (Thermo Fisher Scientific). Soil from initial time-point was not used
157 for DNA extractions.

158

159 **Sequencing of the fungal ITS2 and bacterial V3–V4 regions**

160 For MiSeq sequencing 200 ng of extracted DNA was adjusted to a final concentration of 10 ng μl^{-1}
161 ¹. The fungal Internal Transcribed Spacer (ITS2) and bacterial V3–V4 regions of 16S rDNA from the
162 extracted DNAs were sequenced using Illumina® MiSeq at the Institute of Biotechnology, University
163 of Helsinki.

164 Prior to sequencing, a two-step-PCR was designed by and performed at the Institute of
165 Biotechnology. In the first PCR, extracted DNAs were used as templates and the fungal-specific
166 primers gITS7 and ITS4 (Ihrmark *et al.* 2012) or bacterial-specific primers f341 and r785 (Klindworth
167 *et al.* 2013) containing partial TruSeq adapter sequences at the 5' ends (ATC TAC ACT CTT TCC
168 CTA CAC GAC GCT CTT CCG ATC T and GTG ACT GGA GTT CAG ACG TGT GCT CTT CCG
169 ATC T, respectively) were used. In the second PCR, full-length TruSeq P5 and Index containing P7
170 adapters were used as primers and the products of the first PCR were used as templates.

171

172 **Processing of sequence data**

173 The raw ITS and 16S rDNA sequences were pre-processed at the Institute of Biotechnology and
174 the general read quality was checked with FastQC software
175 (<http://www.bioinformatics.babraham.ac.uk/projects/fastqc/>). Adapter and barcode sequences were
176 cut away using Cutadapt software (Martin 2011). The nucleotide sequence data are available in the
177 NCBI database under Bioproject number PRJNA454770.

178 The sequence data were further filtered and clustered to operational taxonomic units (OTUs) using
179 mothur (version 1.39.5) (Schloss *et al.* 2009). For filtering, denoising and clustering the bacterial
180 sequences to OTUs, the standard operating procedure ((Kozich *et al.* 2013), accessed 2017-01-15)
181 was followed. For filtering, denoising and clustering fungal sequences to OTUs, the pipeline by Sietiö
182 *et al.* (2018) was followed. For identification, bacterial sequences were aligned against the mothur-

183 formatted SILVA-database (release 123, (Quast *et al.* 2012; Yilmaz *et al.* 2014)) as described in the
184 standard operating procedure ((Kozich *et al.* 2013), accessed 2017-01-15) and fungal sequences were
185 aligned against the UNITE-database (UNITE+INSD version 7.1, (Kõljalg *et al.* 2013)) in mothur
186 with classify.seqs.

187 For both bacterial and fungal communities, the sequence data were further de-noised in the R
188 programming environment (R Core Team 2016) with the pipeline suggested by Callahan *et al.* (2016).
189 During de-noising the threshold was set so that those taxa which were present in at least seven samples
190 were kept in analysis and others were discarded. The diversity indices were calculated from the de-
191 noised data with estimate_richness-function after randomly subsampling the data with
192 rarefy_even_depth-function to 49 301 reads per sample with fungal sequences and 20 459 reads per
193 sample with bacterial sequences (McMurdie and Holmes 2013). The obtained fungal taxa were
194 assigned to functional guilds according to the FUNGuild database (Nguyen *et al.* 2016) with
195 metagMisc package (Mikryukov 2017), and only those classifications which had a probability level
196 of “Probable” or higher were kept in further analyses.

197

198 **GeoChip 5.0S microarray**

199 For the GeoChip 5.0S microarray, equal amounts of genomic DNA of each sample were pooled
200 separately within each year and within each sampling site, resulting in a total of three replicates from
201 each treatment in each sampling year (in total 27 samples). A total of 1000 ng of genomic DNA was
202 used for GeoChip at Glomics Inc. There the genomic DNA was mixed with random primers and then
203 labelled with 15 µl of labelling master mix, after which the labelled genomic DNA was purified,
204 dried, and hybridized on the GeoChip 5.0S microarray as previously described (Van Nostrand *et al.*
205 2016). The obtained signal intensities were pre-processed at the Glomics Inc. The signal intensities
206 of each spot were normalized by dividing the signal intensity of that spot with the mean of the whole

207 microarray and multiplied with a constant as described in (Liang *et al.* 2010). The probes were
208 removed as negative if the signal-to-noise ratio was <2 or if the signal intensity was <200. The raw
209 GeoChip microarray data is presented in Supplementary Table 1.

210 The GeoChip microarray data was organized to gene lineages and only fungal and bacterial genes
211 were selected for further analysis, in which fungal and bacterial genes were analyzed separately. The
212 gene diversities from GeoChip were calculated from the probe-level data with diversity and fisher-
213 alpha functions from the vegan-package (Oksanen *et al.* 2017). Different probes from the same gene
214 families were combined by summing them together. For clustering the genes into different
215 subcategories based on their functionality, the preset categories by Glomics Inc were used.

216

217 **Statistical analyses**

218 All the statistical and descriptive analyses for the fungal OTUs were executed in the R
219 programming environment (R Core Team 2016). The level of statistical significance of all analyses
220 was set to $p \leq 0.05$. Significant differences in diversity indices were tested with the non-parametric
221 Kruskal-Wallis test using `kruskal.test`-function from stats package (R Core Team 2016). Statistical
222 significance of the changes detected between the different mesh treatments across the three growing
223 seasons in overall fungal or bacterial communities as well as fungal functional guilds were tested with
224 permutational multivariate analysis of variance (perMANOVA) using 999 permutations with `adonis`-
225 function from vegan package (Oksanen *et al.* 2017). Prior to MANOVA the sequence counts were
226 normalized with the library sizes and log-transformed, and in MANOVA, mesh size, growing season,
227 soil pH, moisture and mass loss (average values represented in Supplementary Table 2) were used as
228 explanatory variables. When performing MANOVA with mesh size as an explanatory variable, the
229 growing season was set to grouping factor.

230 The differences in the soil fungal or bacterial communities between the 1 μm and 1000 μm mesh
231 treatments across the three growing seasons were analyzed with partitioned canonical correspondence
232 analysis (pCCA). The pCCA, where the effect of soil moisture content and sampling area was
233 partitioned out, was conducted with the vegan package (Oksanen *et al.* 2017). For the pCCA,
234 logarithmic transformed abundance data of all fungal OTUs (2566 OTUs) or 3000 most abundant
235 bacterial OTUs were used as variables and mesh size, growing season and soil pH as explanatory
236 variables. The pCCA was visualized with plot.cca-function, and the square root eigenvalues of
237 species and site scores were scaled symmetrically using scaling “symmetric”. The statistical
238 significances of the CCA-axes and explanatory variables were determined with anova.cca-function
239 from vegan package. The species scores of the 25% most abundant and 0.5% of the best fitting OTUs
240 (Supplementary Table 3 for fungi and Supplementary Table 4 for bacteria) were selected with
241 ordiselect-function from goeveg package (Goral and Schellenberg 2017) and visualized in the pCCA.

242 Fungal and bacterial orders, genera and species, and fungal functional guilds responding
243 significantly to the treatment as well as their log₂ changes were identified with DESeq2 package
244 (Love, Huber and Anders 2014). In DESeq2, the level of significant log₂ fold change value was set
245 to ± 1 , adjusted p-value to 0.05, and in addition the change was considered significant only when the
246 abundance of the species or genus was over 1% in at least one of the different mesh treatments. The
247 log₂ changes in DESeq2 were converted to fold changes by calculating 2 to the power of log₂-value
248 (i.e. $2^{\log_2 \text{ change}}$). The Spearman correlations between the bacterial genera or fungal species and the
249 environmental variables, mass loss, soil pH and soil moisture content (Supplementary Table 2), were
250 determined with rcorr-function from Hmisc package (Harrell 2017).

251 For the GeoChip microarray data, the gene diversities of each sample were calculated with R
252 program (R Core Team 2016) using diversity and fisher.alpha-functions from the vegan package
253 (Oksanen *et al.* 2017). The statistical differences in the diversity indices and in the signal intensities

254 between different gene families were determined with the non-parametric Dunn's test (Dinno 2017).
255 The level of statistical significance of the adjusted p-value was set to 0.05.

256

257 **Results**

258 **The mesh treatment effect on mass losses, soil pH and fungal biomass**

259 After the first growing season the pH of soils inside the mesh bags were at similar levels (pH 4.05-
260 4.12) in all the mesh treatments (Supplementary table 2). After the second growing season the soil
261 pH inside the 1000 μm mesh bags started to decline reaching pH 3.86 after the 3rd growing season
262 whereas inside the 50 μm and 1 μm mesh bags the soil pH remained at pH 3.95-4.02 throughout the
263 whole three-year experiment. The mesh size did not affect the soil moisture contents inside the
264 different mesh treatments (Supplementary table 2). However, the soil moisture contents varied
265 between the different growing seasons (Supplementary table 2) and experimental sites (data not
266 shown).

267 During the experiment, the 1000 μm mesh bags had the highest measured mass losses (12 % of
268 the total dry weight lost after 3rd growing season) whereas the mass loss of the 1 μm mesh bags was
269 lowest (9 % of the total dry weight lost after 3rd growing season) (Supplementary table 2), indicating
270 that the microbial SOM degradation activity was lowest in the 1 μm treatments. In addition, the fungal
271 biomass (ergosterol) inside the 1 μm mesh treatments declined almost two-fold between the first and
272 third growing seasons whereas in the 1000 μm mesh treatments the fungal biomass increased during
273 the experiment (Supplementary table 2). Within the 1000 μm and 50 μm mesh treatments, plant fine
274 roots grew inside the mesh bags, and after the 3rd growing season, the roots accounted for up to 2%
275 of the total fresh weight of the 1000 μm mesh bags (Supplementary table 2). No root ingrowth was
276 detected with the 1 μm mesh bags.

277

278 **Overall microbial community diversity**

279 From samples describing the total microbial community of the mesh bags, a total of 16 848 032
280 raw fungal ITS2 sequences and 15 259 602 raw bacterial 16S rDNA sequences were obtained. After
281 quality control and de-noising, 11 054 791 high-quality and non-chimeric fungal sequences and 11
282 321 704 bacterial sequences remained (Table 1 a, b). The fungal sequences were divided into 2566
283 fungal OTUs and the bacterial sequences were divided into 6537 bacterial OTUs. The alpha-
284 diversities of neither fungal nor bacterial communities between 1000 μm , 50 μm and 1 μm mesh
285 treatments differed significantly (Table 1 a,b), but based on the Fisher indices, both the fungal and
286 bacterial species richness were the highest after the 1st growing season and decreased during the
287 experimental time in all mesh sizes ($p \leq 0.01$, Kruskal-Wallis). In addition, based on the Shannon and
288 Inverse Simpson indices, the detected species in the bacterial communities were more unevenly
289 distributed after the 1st growing season than after 2nd and 3rd growing seasons ($p \leq 0.001$, Kruskal-
290 Wallis) (Table 1 b).

291

292 **Changes in fungal community**

293 The fungal community structures within each mesh size changed during the experimental time (p
294 ≤ 0.001 for each mesh treatment with perMANOVA). Differences in soil moisture content and soil
295 pH explained the observed changes in the fungal community structures ($p \leq 0.001$ for each treatment
296 with perMANOVA). Also, the fungal community structures between the three sampling areas
297 differed from each other ($p \leq 0.001$ with perMANOVA, data not shown). Within each growing
298 season, the fungal community structures between 1000 μm and 1 μm mesh treatments differed from
299 each other ($p \leq 0.01$ with perMANOVA, Fig. 2a), but not from 50 μm treatment.

300 The fungal OTUs were divided into seven phyla: Basidiomycota (62% of fungal sequences),
301 Ascomycota (29% of fungal sequences), Mucoromycota (5.4% of fungal sequences), Rozellomycota,
302 Glomeromycota, Zoopagomycota and Chytridiomycota. The most abundant fungal phylum
303 Basidiomycota harbored altogether 31 orders (Table 2). From these, Agaricales was more abundant
304 in the 1 μm mesh treatment than in the 1000 μm treatment ($p\text{-adj} \leq 0.01$ with DESeq2), whereas
305 Boletales was more abundant in the 1000 μm mesh than in the other treatments ($p\text{-adj} \leq 0.001$ with
306 DESeq2). The abundances of ECM fungi from genera *Russula* (6.7% of all sequences), *Piloderma*
307 (9.9% of all sequences) and *Tylospora* (9.2% of all sequences) increased during the experiment in all
308 the mesh sizes ($p\text{-adj} \leq 0.001$ for *Piloderma* with DESeq2, Table 2). In contrast, the abundances of
309 ECM *Lactarius* (14.2% of all sequences) decreased during the experiment in all mesh sizes (Table
310 2).

311 Significant order, genus and species-level differences between the 1000 μm and 1 μm as well as
312 1000 μm and 50 μm mesh treatments were also detected (Table 2). The ECM fungal genus *Suillus*
313 (1.6% of sequences) was more abundant in 1000 μm mesh than in 50 μm or 1 μm mesh ($p\text{-adj} \leq 0.001$
314 with DESeq2). Likewise, the ECM *Suillus bovinus* had a similar trend, and especially after the 3rd
315 growing season it was more abundant in the 1000 μm mesh than in the other mesh sizes ($p\text{-adj} \leq 0.05$
316 with DESeq2). Also, *Inocybe* and *Oidiodendron maius* were more abundant in the 1000 μm mesh
317 than in 50 μm or 1 μm mesh treatments after the 3rd growing season ($p\text{-adj} \leq 0.01$ with DESeq2).
318 Contrarily, the ECM genus *Cortinarius* was more abundant in the 1 μm than in 1000 μm mesh
319 treatment ($p\text{-adj} \leq 0.001$ with DESeq2). In addition, the ECM *Russula decolorans*, was more
320 abundant in 50 μm and 1 μm mesh treatments than in 1000 μm ($p\text{-adj} \leq 0.05$ with DESeq2). The
321 abundance of the saprotroph *Sistotremastrum* increased between the 1st and 3rd growing seasons in
322 the 1000 μm mesh treatment whereas in the 50 μm and 1 μm treatments its abundance decreased ($p\text{-}$
323 $\text{adj} \leq 0.05$ with DESeq2).

324

325 Functional distribution of the fungal community

326 A total of 1118 fungal OTUs (43.6% of all fungal OTUs and 68.6% of sequences) could be
327 assigned to different trophic modes (Fig. 3). Symbiotrophs were the most abundant fungal trophic
328 mode covering 44–60% of the assigned sequence reads. Symbiotrophs consisted mainly of
329 ectomycorrhizal (ECM) fungi whereas ericoid mycorrhizal fungi were detected less, and as expected
330 arbuscular mycorrhizal fungi were in minority across all the treatments. Saprotrophic activity
331 possessing fungal OTUs covered 6.1–14% of the sequence reads of the different treatments.
332 Pathotrophic activity possessing fungal OTUs covered 4.7–8.6% of the sequence reads and their
333 proportion declined during the experiment in all the mesh treatments.

334 Although the amount of all fungal biomass declined in 1 μ m mesh treatment over the three growing
335 seasons compared to 1000 μ m mesh treatment (Supplementary table 2), we detected also differences
336 in the proportional distribution of all sequences per sample to different fungal functional guilds
337 between the different mesh treatments. Overall, the percentage of plant pathogens, universal
338 saprotrophs and endophytes from all sequences per sample was 1.1–2.4-fold higher (p-adj \leq 0.05 with
339 DESeq2, data not shown) in 1000 μ m mesh treatment than in 1 μ m mesh. The percentage of wood
340 saprotrophs from all sequences per sample in 1000 μ m mesh treatment was 1.5-fold higher (p-adj \leq
341 0.05 with DESeq2, data not shown) than in 50 μ m and 1 μ m mesh. Contrarily, the proportion of
342 “undefined saprotrophs” was 1.3-fold higher in 1 μ m mesh treatments (p-adj \leq 0.05 with DESeq2,
343 data not shown) than in 1000 μ m mesh. The overall proportions of different fungal guilds from all
344 the sequences per sample did not differ with statistical significance between the 50 μ m and 1 μ m
345 mesh treatments.

346

347 **Changes in bacterial community**

348 The bacterial community structures within each mesh size changed significantly during the
349 experiment (p \leq 0.001 for each mesh treatment with perMANOVA). Differences in soil moisture

350 content and soil pH influenced the bacterial community structures ($p \leq 0.001$ with perMANOVA).
351 Within each growing season, the bacterial communities between 1000 μm and 1 μm treatments
352 differed from each other ($p \leq 0.05$ with perMANOVA, Fig. 2b), but were similar with the 50 μm
353 treatment. The bacterial community structures between the three sampling areas differed from each
354 other ($p \leq 0.05$ with perMANOVA, data not shown).

355 The bacterial orders and genera correlating significantly with the soil properties (see
356 Supplementary Table 2) belonged mainly to the classes Acidobacteria, Alphaproteobacteria,
357 Deltaproteobacteria, Actinobacteria and Sphingobacteriia (Table 3). The abundances of class
358 Sphingobacteriia (2.6% of sequences), orders Rhizobiales (15.7% of all sequence-reads),
359 Caulobacterales (2.1% of sequences), as well as genera *Rhizomicrobium*, *Phenylobacterium*, and
360 *Mucilaginibacter* correlated with the soil moisture content and the mass losses of the mesh bags with
361 statistical significance (Table 3). The order Myxococcales (2.7% of sequences), genera *Haliangium*
362 and *Acidobacterium* correlated with the soil moisture content and pH. In addition, the order
363 Rhodospirillales (7.2% of the sequences) correlated significantly with the soil pH and mass losses of
364 the mesh bags, whereas the order Acidobacteriales (15.9% of sequences) and the genus *Sorangium*
365 correlated only with the soil pH with statistical significance.

366

367 **The potential functionality of the microbial communities**

368 A total of 2717 fungal gene probes and 30 183 bacterial gene probes were detected from the
369 samples using the GeoChip 5.0S microarray. Gene probes originating from archaea and viruses were
370 omitted from this analysis. The alpha-diversities between the different mesh treatments did not differ
371 with each other (data not shown). The potential functional fungal and bacterial gene pools did not
372 differ between the treatments, and the growing season was the most significant factor explaining the

373 differences in the potential functional gene pool structures of both fungi and bacteria ($p \leq 0.05$ with
374 perMANOVA, Supplementary Table 5a,b).

375

376

377 **Discussion**

378 We found that the three mesh treatments caused different changes to the fungal community
379 structure inside the mesh bags and modulated also the bacterial community composition during three
380 growing seasons. Contrary to our original hypothesis, in the 1 μm mesh bags, where access of plant
381 roots and external fungal hyphae was restricted, the proportion of ECM fungi remained dominant
382 when comparing to the total fungal community inside the mesh treatment. However, the total fungal
383 ergosterol concentration declined inside the 1 μm mesh bags over the three growing seasons
384 indicating a decline also in the fungal biomass (Supplementary table 2). Thus, despite of the relative
385 dominance of ECM fungi in the 1 μm mesh treatments (Fig. 3), the absolute amount of ECM biomass
386 likely declined when compared to other mesh treatments. As the changes in the fungal and bacterial
387 community structures were modest (Fig. 2), our results indicate that members of the soil microbial
388 community can survive from rather short-term environmental changes.

389 Both saprotrophs and ECM fungi can degrade plant biomass through Fenton chemistry (Lindahl
390 and Tunlid 2015; Shah *et al.* 2016; Op De Beeck *et al.* 2018) and by producing plant cell wall
391 degrading enzymes (Lundell, Mäkelä and Hildén 2010; Lindahl and Tunlid 2015). As more efficient
392 degraders, true saprotrophs generally dominate the boreal forest litter layers whereas the O_F and O_H
393 layers are dominated by ECM fungi (Lindahl *et al.* 2007; Santalahti *et al.* 2016). This separation is
394 likely maintained by the competition for nutrients between saprotrophs and mycorrhiza and the ECM
395 fungi are suggested to outcompete the saprotrophs via access to C provided by the plants (Gadgil and

396 Gadgil 1971). Based on the theory behind the “Gadgil effect”, we hypothesized that in the 1 μm
397 treatments the internal fungal community structure would change, the relative proportion of the soil
398 originally inhabiting saprotrophs would increase, and the proportion of mycorrhiza would decrease.
399 Contrary to our hypothesis and previous findings (Gadgil and Gadgil 1971; Lindahl, de Boer and
400 Finlay 2010; Bödeker *et al.* 2016), in 1 μm mesh bags internal community the proportion of
401 saprotrophs did not increase (Fig. 3). Contrary to previous experiments, in our experiment the soil
402 from O_F and O_H layers that was used for constructing the mesh bags was sieved to remove fine roots
403 and all particles larger than 4 mm leaving a limited amount of plant biomass to serve as a substrate
404 for the microbes. Thus, the microbes inside the 1 μm mesh treatment likely suffered from energy
405 depletion during the experiment. Furthermore, in the 1000 μm mesh treatment, the fine roots could
406 grow inside the mesh bags and the amount of fresh plant roots accounted for up to 2% of the total
407 fresh weight of the mesh bags after the last growing season (Supplementary table 2). Presumably, the
408 plant root exudates and litter had been used as easily-utilizable substrates by the saprotrophs, and thus
409 possibly explain the increase of saprotrophs in the 1000 μm mesh treatment.

410 In our study, the abundance of the ECM *Russula* and *Cortinarius* increased in the 1 μm mesh
411 treatment and decreased in the 1000 μm mesh treatment (Table 2). Most ECM are slow growing but
412 tend to dominate the decomposition of recalcitrant SOM (Fontaine, Mariotti and Abbadie 2003). Even
413 though the saprotrophic machinery of ECM is less efficient than that of true saprotrophs (Kohler *et*
414 *al.* 2015), this affinity towards recalcitrant SOM may have given some ECM fungi an advantage
415 against those saprotrophs that originally inhabited the organic soil placed inside the 1 μm mesh bags.
416 Although the ECM fungi scavenge SOM mainly for N (Lindahl and Tunlid 2015), based on the “Plan
417 B hypothesis” mycorrhizal fungi may decompose SOM to acquire C when the photosynthetic-C flow
418 is insufficient (Talbot, Allison and Treseder 2008). Also, other studies have indicated that the
419 outcome of competition between ECM and saprotrophic fungi is dependent on the quality of the
420 substrate (Lindahl *et al.* 1999; Lindahl, Stenlid and Finlay 2001), and in a field-study Bödeker *et al.*

421 (2016) showed that sterilized humus was colonized more eagerly by mycorrhizal fungi than
422 saprotrophs after two growing seasons. In addition, the degradation of humus is suggested to be
423 unprofitable for saprotrophs (Baldrian 2009). Thus, our results of ECM dominance in the 1 μm
424 treatment combined with the previous studies indicate different niche and substrate preferences
425 between mycorrhizal and saprotrophic fungi and support the hypothesis by Averill & Hawkes (2016)
426 and Fernandez & Kennedy (2016) that the appearance of “Gadgil effect” is substrate dependent.

427 Since plant roots and their exudates as well as root associated fungi can affect the bacterial growth
428 (de Boer *et al.* 2005), we hypothesized that the different mesh treatments would cause changes also
429 to the soil bacterial communities. However, the bacterial populations were most affected by the soil
430 pH and soil moisture content rather than the mesh treatments (Fig. 2, Table 3). These results are in
431 line with previous findings that the bacterial communities in soils are sensitive to soil chemistry and
432 pH (Männistö, Tirola and Häggblom 2007; Jeanbille *et al.* 2016). However, previous studies have
433 shown that the pH of organic soil from O_F and O_H layers is strongly influenced by the presence of
434 plant roots and their exudates since the pH of unplanted soil is over pH 4.5 whereas in the presence
435 of boreal plant roots the pH is typically around 4.0 (Adamczyk *et al.* 2016; Kieloaho *et al.* 2016).
436 Also, in our study the pH of 1 μm mesh bags remained higher than the pH of 1000 μm bags across
437 the three growing seasons (Supplementary table 2). The observed changes in soil pH and the
438 significance of the pH to the bacterial community structures may be mediated by the exclusion of
439 plant roots.

440 We hypothesized that the shift in microbial community structures would be also related to their
441 potential functionality, and we investigated this with DNA-based GeoChip 5.0S. However, we did
442 not detect significant differences between the treatments. Instead, inside each mesh treatment the
443 functional gene pools changed differently during the three-year experiment. Since both bacteria and
444 fungi typically contain multiple copies of genes encoding for enzymes related to cellulose,
445 hemicelluloses and lignin degradation (Floudas *et al.* 2012; López-Mondéjar *et al.* 2016), it is

446 probable that only drastic changes in microbial community structures would affect the potential
447 functionality of the community. However, the structure of the active microbial community in boreal
448 forest soil can differ highly from that of the total microbial community (Baldrian *et al.* 2012) and the
449 metabolic activity of microorganisms may decrease with decreasing nutrient availability (Stenström,
450 Svensson and Johansson 2001; Wright *et al.* 2002; Nitsche *et al.* 2012). It is likely that in our study
451 the plant biomass degradation related genes were differently expressed in the 1000 μm , 50 μm , and
452 1 μm treatments.

453 In this work, we assessed the total fungal and bacterial DNA from the mesh bags containing both
454 living and dead microbes as well as spores. Based on the lower mass loss and lower fungal biomass
455 in the 1 μm treatment compared to the other treatments (Supplementary table 2), it is probable that
456 microorganisms have been less active or dead in the 1 μm treatment than in the other mesh sizes due
457 to possible nutrient depletion. The depletion of nutrients and especially easily-utilizable C may have
458 caused the soil microbes in 1 μm mesh bags to lower their metabolic rates. When encountering rather
459 short environmental disturbances, such as nutrient depletion, microbes can adapt to it by going into a
460 metabolically inactive state and recover from it when there are more nutrients available (Stenström,
461 Svensson and Johansson 2001; Jones and Lennon 2010; Lennon and Jones 2011). In our experiment,
462 the possibly dormant or metabolically less-active microbes, as well as spores, might have persisted
463 longer inside the 1 μm mesh bags than they would normally in natural boreal forest soils since they
464 were protected from soil macro- and meso-fauna. In addition, some microbes can produce propagules
465 that are more resistant in the soil than others, and these may have contributed also in our experiment
466 to the DNA-profiles of the total microbial communities detected in different mesh treatments. Thus,
467 a prolonged mesh treatment could cause more drastic changes to microbial communities, and further
468 investigations of shifts in both RNA- and DNA-profiles comparing active and total microbial
469 communities are needed.

470

471

472 **Conclusions**

473 The manipulation of the presence of plant roots and external fungal hyphae in mesh bags filled
474 with homogenized soil over three growing seasons caused moderate changes to both fungal and
475 bacterial community structures. Our results also indicate that the boreal forest soil microbial
476 community can survive from relatively short-term environmental changes. Contrary to the theory
477 behind the “Gadgil effect”, the internal community of mesh bags restricting the entrance of both plant
478 roots and external fungal hyphae were dominated by ECM fungi rather than saprotrophic fungi and
479 the total fungal biomass declined significantly. It is noteworthy, that although the decline in ECM
480 biomass was expected, saprotrophic fungi did not occupy the “free niche” in the 1 μm bags. Thus, it
481 seems that appearance of the “Gadgil effect” is substrate dependent and might reflect the different
482 niche preferences of the ECM and saprotrophic fungal guilds. However, to determine if the spatial
483 separation of ECM and saprotrophs is due to antagonistic interactions or ecological niche preference,
484 we propose that in future studies the long-term competitive interactions between ECM and
485 saprotrophic guilds should be compared on different substrates containing for example sieved organic
486 soil, organic soil mixed with litter, different litter qualities as well as root fragments. In addition, our
487 results suggest that the plant roots and their exudates are important in shaping the microbial
488 community structure and functionality in boreal forest soils. To confirm our findings, a more detailed
489 study assessing the responses of both the total and active microbial community structures to long-
490 term manipulations of the presence of plant roots in organic O_F and O_H soil layers is required.

491

492 **Acknowledgements**

493 This work was financially supported by Academy of Finland (grant numbers 263858, 292699),
494 Academy of Finland Centre of Excellence (grant number 307331), University of Helsinki Doctoral
495 Program in Microbiology and Biotechnology (MBDP), The Finnish Society of Forest Science, Niemi
496 Foundation, The Finnish Cultural Foundation, research funding for Jiangsu Specially-Appointed
497 Professor (project 165010015) and Priority Academic Program Development of Jiangsu Higher
498 Education Institutions. We acknowledge Prof. Mari Pihlatie, Dr. Antti-Jussi Kieloaho and MSc Elisa
499 Halmeenmäki for their contribution to the sampling. We are thankful for Dr. Bartosz Adamczyk for
500 providing helpful comments on the manuscript.

501

502 **Conflict of interest**

503 There are no conflicts of interest related to this work.

504

505

506 **References**

507 Adamczyk B, Ahvenainen A, Sietiö O-M *et al.* The contribution of ericoid plants to soil nitrogen
508 chemistry and organic matter decomposition in boreal forest soil. *Soil Biol Biochem*
509 2016;**103**:394–404.

510 Averill C, Hawkes C V. Ectomycorrhizal fungi slow soil carbon cycling. *Ecol Lett* 2016;**19**:937–47.

511 Baldrian P. Ectomycorrhizal fungi and their enzymes in soils: Is there enough evidence for their role
512 as facultative soil saprotrophs? *Oecologia* 2009;**161**:657–60.

513 Baldrian P, Kolařík M, Štursová M *et al.* Active and total microbial communities in forest soil are
514 largely different and highly stratified during decomposition. *ISME J* 2012;**6**:248–58.

515 Op De Beeck M, Troein C, Peterson C *et al.* Fenton reaction facilitates organic nitrogen acquisition
516 by an ectomycorrhizal fungus. *New Phytol* 2018;**218**:335–43.

517 Bödeker ITM, Lindahl BD, Olson Å *et al.* Mycorrhizal and saprotrophic fungal guilds compete for
518 the same organic substrates but affect decomposition differently. *Funct Ecol* 2016;**30**:1967–78.

519 de Boer W, Folman LB, Summerbell RC *et al.* Living in a fungal world: Impact of fungi on soil
520 bacterial niche development. *FEMS Microbiol Rev* 2005;**29**:795–811.

521 Callahan BJ, Sankaran K, Fukuyama JA *et al.* Bioconductor Workflow for Microbiome Data
522 Analysis: from raw reads to community analyses. *F1000Research* 2016;**5**:1492.

523 DeLuca TH, Boisvenue C. Boreal forest soil carbon: Distribution, function and modelling. *Forestry*
524 2012;**85**:161–84.

525 Dinno A. dunn.test: Dunn’s Test of Multiple Comparisons Using Rank Sums. 2017. Available from:
526 <https://cran.r-project.org/package=dunn.test>

527 Fernandez CW, Kennedy PG. Revisiting the ‘Gadgil effect’: do interguild fungal interactions control
528 carbon cycling in forest soils? *New Phytol* 2016;**209**:1382–94.

529 Floudas D, Binder M, Riley R *et al.* The Paleozoic Origin of Enzymatic Lignin Decomposition
530 Reconstructed from 31 Fungal Genomes. *Science* 2012;**336**:1715–9.

531 Fontaine S, Mariotti A, Abbadie L. The priming effect of organic matter: A question of microbial
532 competition? *Soil Biol Biochem* 2003;**35**:837–43.

533 Frostegard A, Bååth E. The use of phospholipid fatty acid analysis to estimate bacterial and fungal
534 biomass in soil. *Biol Fertil Soils* 1996;**22**:59–65.

- 535 Gadgil RL, Gadgil PD. Mycorrhiza and Litter Decomposition. *Nature* 1971;**233**:133–133.
- 536 Gadgil RL, Gadgil PD. Suppression of litter decomposition by mycorrhizal roots of *Pinus radiata*.
537 *New Zeal J For Sci* 1975;**5**:33–41.
- 538 Goral F, Schellenberg J. goeveg: Functions for Community Data and Ordinations. 2017.
- 539 Harrell FEJ. Hmisc: Harrell Miscellaneous. 2017. Available from: [https://cran.r-](https://cran.r-project.org/package=Hmisc)
540 [project.org/package=Hmisc](https://cran.r-project.org/package=Hmisc)
- 541
- 542 Ihrmark K, Bödeker ITM, Cruz-Martinez K *et al.* New primers to amplify the fungal ITS2 region--
543 evaluation by 454-sequencing of artificial and natural communities. *FEMS Microbiol Ecol*
544 2012;**82**:666–77.
- 545 Izumi H, Finlay RD. Ectomycorrhizal roots select distinctive bacterial and ascomycete communities
546 in Swedish subarctic forests. *Environ Microbiol* 2011;**13**:819–30.
- 547 Jeanbille M, Buée M, Bach C *et al.* Soil Parameters Drive the Structure, Diversity and Metabolic
548 Potentials of the Bacterial Communities Across Temperate Beech Forest Soil Sequences. *Microb*
549 *Ecol* 2016;**71**:482–93.
- 550 Jones SE, Lennon JT. Dormancy contributes to the maintenance of microbial diversity. *Proc Natl*
551 *Acad Sci U S A* 2010;**107**:5881–6.
- 552 Kieloaho A-J, Pihlatie M, Dominguez Carrasco M *et al.* Stimulation of soil organic nitrogen pool:
553 The effect of plant and soil organic matter degrading enzymes. *Soil Biol Biochem* 2016;**96**:97–
554 106.
- 555 Klindworth A, Pruesse E, Schweer T *et al.* Evaluation of general 16S ribosomal RNA gene PCR
556 primers for classical and next-generation sequencing-based diversity studies. *Nucleic Acids Res*

557 2013;**41**:1–11.

558 Kohler A, Kuo A, Nagy LG *et al.* Convergent losses of decay mechanisms and rapid turnover of
559 symbiosis genes in mycorrhizal mutualists. *Nat Genet* 2015;**47**:410–5.

560 Kõljalg U, Nilsson RH, Abarenkov K *et al.* Towards a unified paradigm for sequence-based
561 identification of fungi. *Mol Ecol* 2013;**22**:5271–7.

562 Kozich JJ, Westcott SL, Baxter NT *et al.* Development of a dual-index sequencing strategy and
563 curation pipeline for analyzing amplicon sequence data on the MiSeq Illumina sequencing
564 platform. *Appl Environ Microbiol* 2013;**79**:5112–20.

565 Kuzyakov Y, Domanski G. Carbon input by plants into the soil. Review. *J Plant Nutr Soil Sci*
566 2000;**163**:421–31.

567 Lennon JT, Jones SE. Microbial seed banks: the ecological and evolutionary implications of
568 dormancy. *Nat Rev Microbiol* 2011;**9**:119–30.

569 Liang Y, He Z, Wu L *et al.* Development of a common oligonucleotide reference standard for
570 microarray data normalization and comparison across different microbial communities. *Appl*
571 *Environ Microbiol* 2010;**76**:1088–94.

572 Lindahl BD, de Boer W, Finlay RD. Disruption of root carbon transport into forest humus stimulates
573 fungal opportunists at the expense of mycorrhizal fungi. *ISME J* 2010;**4**:872–81.

574 Lindahl BD, Ihrmark K, Boberg J *et al.* Spatial separation of litter decomposition and mycorrhizal
575 nitrogen uptake in a boreal forest. *New Phytol* 2007;**173**:611–20.

576 Lindahl BD, Stenlid J, Finlay R. Effects of resource availability on mycelial interactions and ³²P
577 transfer between a saprotrophic and an ectomycorrhizal fungus in soil microcosms. *FEMS*
578 *Microbiol Ecol* 2001;**38**:43–52.

579 Lindahl BD, Stenlid J, Olsson S *et al.* Translocation of ³²P between interacting mycelia of a wood-
580 decomposing fungus and ectomycorrhizal fungi in microcosm systems. *New Phytol*
581 1999;**144**:183–93.

582 Lindahl BD, Taylor AFS, Finlay RD. Defining nutritional constraints on carbon cycling in boreal
583 forests – towards a less “phytcentric” perspective. *Plant Soil* 2002;**242**:123–35.

584 Lindahl BD, Tunlid A. Ectomycorrhizal fungi - potential organic matter decomposers, yet not
585 saprotrophs. *New Phytol* 2015;**205**:1443–7.

586 López-Mondéjar R, Zühlke D, Becher D *et al.* Cellulose and hemicellulose decomposition by forest
587 soil bacteria proceeds by the action of structurally variable enzymatic systems. *Sci Rep*
588 2016;**6**:1–12.

589 Love MI, Huber W, Anders S. Moderated estimation of fold change and dispersion for RNA-seq data
590 with DESeq2. *Genome Biol* 2014;**15**:550.

591 Lundell TK, Mäkelä MR, Hildén K. Lignin-modifying enzymes in filamentous basidiomycetes -
592 Ecological, functional and phylogenetic review. *J Basic Microbiol* 2010;**50**:5–20.

593 Männistö MK, Tirola M, Häggblom MM. Bacterial communities in Arctic fields of Finnish Lapland
594 are stable but highly pH-dependent. *FEMS Microbiol Ecol* 2007;**59**:452–65.

595 Martin M. Cutadapt removes adapter sequences from high-throughput sequencing reads.
596 *EMBnet.journal* 2011;**17**:10.

597 McMurdie PJ, Holmes SP. phyloseq: An R package for reproducible interactive analysis and graphics
598 of microbiome census data. *PLoS One* 2013;**8**:e61217.

599 Mikryukov V. metagMisc: Miscellaneous functions for metagenomic analysis. 2017. Available from:
600 <https://github.com/vmikk/metagMisc>

601 Näsholm T, Kielland K, Ganeteg U. Uptake of organic nitrogen by plants. *New Phytol* 2009;**182**:31–
602 48.

603 Nguyen NH, Song Z, Bates ST *et al.* FUNGuild: An open annotation tool for parsing fungal
604 community datasets by ecological guild. *Fungal Ecol* 2016;**20**:241–8.

605 Nitsche BM, Jørgensen TR, Akeroyd M *et al.* The carbon starvation response of *Aspergillus niger*
606 during submerged cultivation : Insights from the transcriptome and secretome. *BMC Genomics*
607 2012;**13**:1–23.

608 Van Nostrand J, Yin H, Wu L *et al.* Hybridization of Environmental Microbial Community Nucleic
609 Acids by GeoChip. In: Martin F, Uroz S (eds.). *Methods in Molecular Biology - Microbial*
610 *Environmental Genomics*. Vol 1399. New York: Springer Science & Business Media, 2016,
611 183–96.

612 Oksanen J, Blanchet FG, Friendly M *et al.* vegan: Community Ecology Package. 2017. Available
613 from: <https://cran.r-project.org/package=vegan>

614 Quast C, Pruesse E, Yilmaz P *et al.* The SILVA ribosomal RNA gene database project: improved
615 data processing and web-based tools. *Nucleic Acids Res* 2012;**41**:D590–6.

616 R Core Team. R: A language and environment for statistical computing. *R Found Stat Comput*
617 *Vienna, Austria* 2016. Available from: <https://www.r-project.org/>.

618 Santalahti M, Sun H, Jumpponen A *et al.* Vertical and seasonal dynamics of fungal communities in
619 boreal Scots pine forest soil of fungi in boreal forests. *FEMS Microbiol Ecol* 2016;**92**:1–31.

620 Schloss PD, Westcott SL, Ryabin T *et al.* Introducing mothur: open-source, platform-independent,
621 community-supported software for describing and comparing microbial communities. *Appl*
622 *Environ Microbiol* 2009;**75**:7537–41.

623 Schulten R, Schnitzer M. The chemistry of soil organic nitrogen : a review. *Agriculture* 1998;**26**:1–

- 624 15.
- 625 Shade A, Peter H, Allison SD *et al.* Fundamentals of microbial community resistance and resilience.
626 *Front Microbiol* 2012;**3**:417.
- 627 Shah F, Nicolás C, Bentzer J *et al.* Ectomycorrhizal fungi decompose soil organic matter using
628 oxidative mechanisms adapted from saprotrophic ancestors. *New Phytol* 2016;**209**:1705–19.
- 629 Sietiö O-M, Tuomivirta T, Santalahti M *et al.* Ericoid plant species and *Pinus sylvestris* shape fungal
630 communities in their roots and surrounding soil. *New Phytol* 2018;**218**:738–51.
- 631 Skyring GW, Quadling C. Soil bacteria: comparisons of rhizosphere and nonrhizosphere populations.
632 *Can J Microbiol* 1969;**15**:473–88.
- 633 Smith SE, Read DJ. *Mycorrhizal Symbiosis*. 3rd Edition. Cambridge, UK: Academic Press, 2008.
- 634 Stenström J, Svensson K, Johansson M. Reversible transition between active and dormant microbial
635 states in soil. *FEMS Microbiol Ecol* 2001;**36**:93–104.
- 636 Talbot JM, Allison SD, Treseder KK. Decomposers in disguise: mycorrhizal fungi as regulators of
637 soil C dynamics in ecosystems under global change. *Funct Ecol* 2008;**22**:955–63.
- 638 Timonen S, Jørgensen KS, Haahtela K *et al.* Bacterial community structure at defined locations of
639 *Pinus sylvestris* - *Suillus bovinus* and *Pinus sylvestris* - *Paxillus involutus* mycorrhizospheres in
640 dry pine forest humus and nursery peat. *Can J Microbiol* 1998;**44**:499–513.
- 641 Timonen S, Sen R. Heterogeneity of fungal and plant enzyme expression in intact Scots pine – *Suillus*
642 *bovinus* and – *Paxillus involutus* mycorrhizospheres developed in natural forest humus. *New*
643 *Phytol* 1998;**138**:355–66.
- 644 Timonen S, Sinkko H, Sun H *et al.* Ericoid Roots and Mycospheres Govern Plant-Specific Bacterial
645 Communities in Boreal Forest Humus. *Microb Ecol* 2017;**73**:939–53.

646 Wallander H, Nilsson LO, Hagerberg D *et al.* Estimation of the biomass and seasonal growth of
647 external mycelium of ectomycorrhizal fungi in the field. *New Phytol* 2001;**151**:753–60.

648 Wright DP, Johansson T, Quéré A Le *et al.* Spatial patterns of gene expression in the extramatrical
649 mycelium and mycorrhizal root tips formed by the ectomycorrhizal fungus *Paxillus involutus* in
650 association with birch (*Betula pendula*) seedlings in soil microcosms. *New Phytol*
651 2002;**167**:579–96.

652 Yilmaz P, Parfrey LW, Yarza P *et al.* The SILVA and “All-species Living Tree Project (LTP)”
653 taxonomic frameworks. *Nucleic Acids Res* 2014;**42**:D643–8.

654

655

Figures:

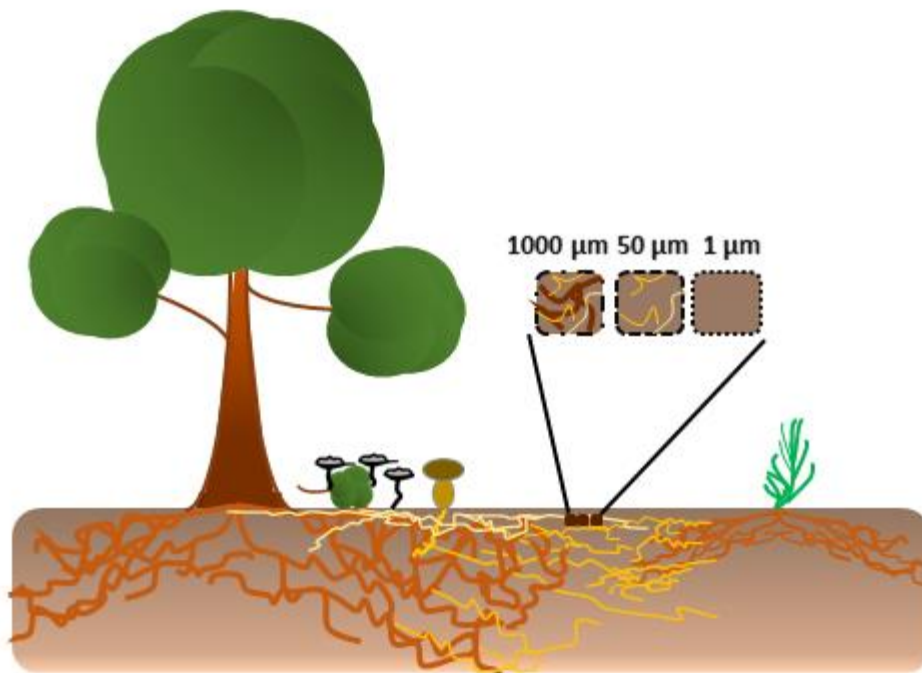


Figure 1. Schematic representation of the experimental setup where the mesh bags with three different pore sizes were buried between organic and mineral soil horizons. 1000 μm mesh size allowed penetration of both fungal hyphae and fine roots, 50 μm mesh size allowed fungal hyphae to penetrate but restricted plant roots, and 1 μm mesh size prevented the entrance of both fungal hyphae and plant roots. For determining the microbial community profiles, 18 mesh bags from each treatment were collected after 1st, 2nd and 3rd growing season.

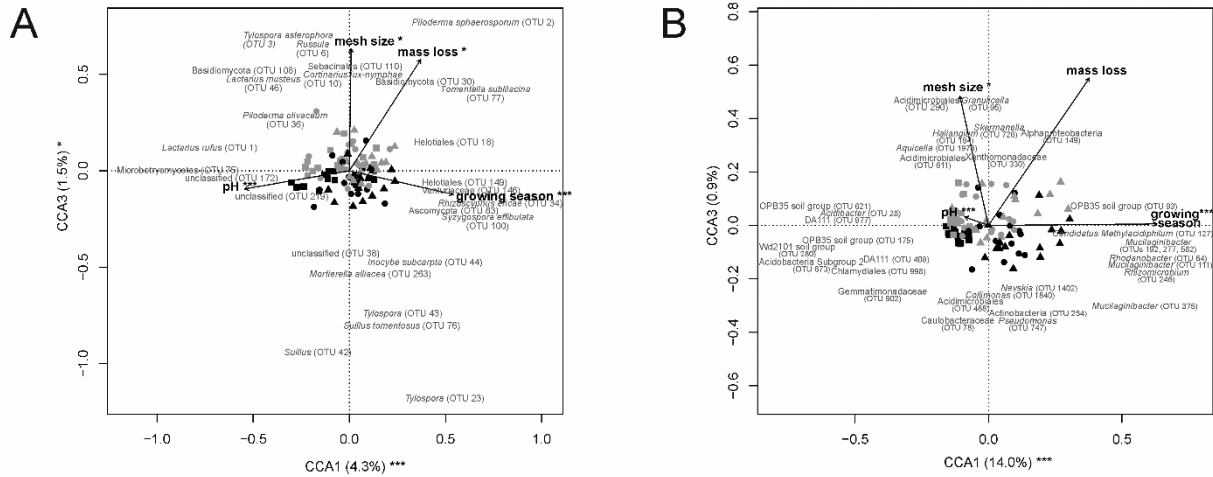


Figure 2. Partitioned canonical correspondence analysis, where the soil moisture content and sampling area have been partitioned out, representing the differences between a) fungal communities and b) bacterial communities of the 1000 μm and 1 μm mesh bags during the three growing seasons. The 1000 μm mesh treatment is visualized with gray and the 1 μm mesh treatment is visualized with black color. The different growing seasons are represented with square (■) for 1st growing season, circle (●) for 2nd growing season, and triangle (▲) for 3rd growing season. The species scores of the 25% most abundant and 0.5% of the best fitting fungal OTUs are visualized (Supplementary Table 3 for fungi and Supplementary Table S4 for bacteria). The statistical significances of the explanatory variables and axes are presented; * $p \leq 0.05$, ** $p \leq 0.01$, *** $p \leq 0.001$. The soil moisture content and sampling area explained 8.3 % of variation in case of fungal community and 10 % of variation in case of bacterial community. The fungal and bacterial community structures between 1000 μm and 1 μm mesh treatments differed from each other ($p \leq 0.01$ for fungal communities and $p \leq 0.05$ for bacterial communities with perMANOVA). Additionally, both the fungal and bacterial community structures within each mesh size changed significantly during the experiment ($p \leq 0.001$ with perMANOVA).

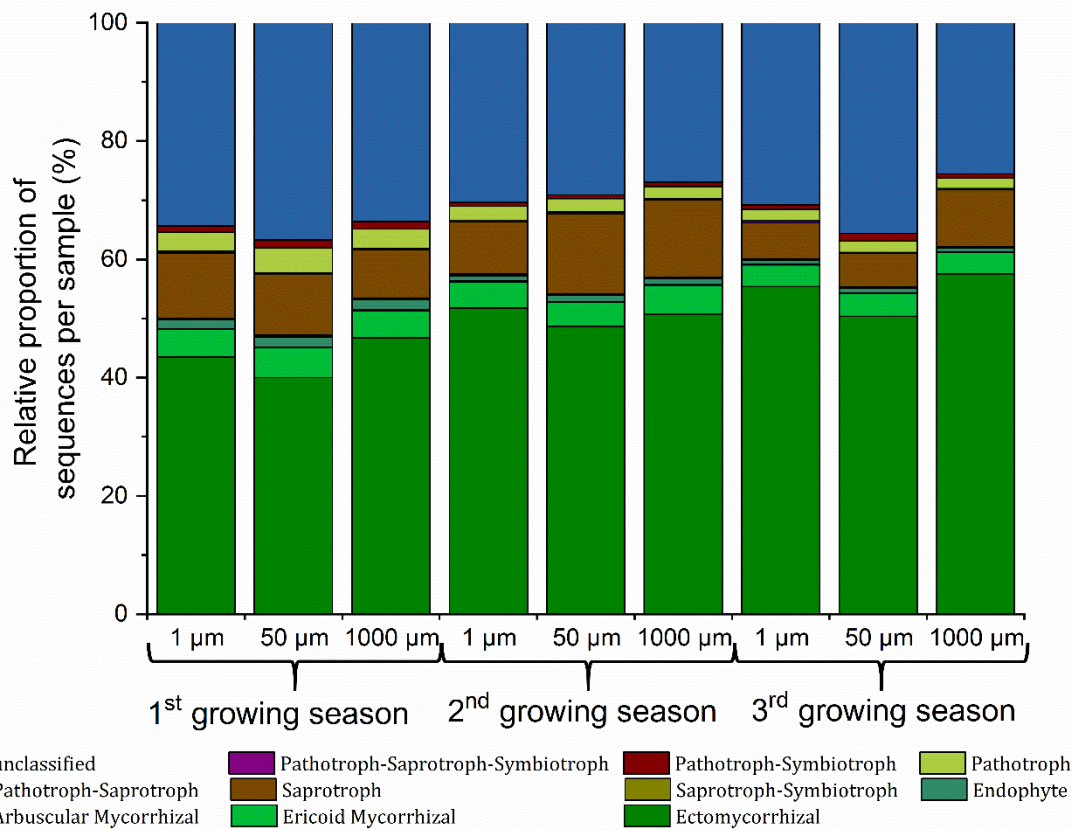


Figure 3. The relative proportion (percentages of the total sequence count per sample) of fungal OTUs in different trophic modes. Within the fungal functional guilds, the proportion of “plant pathogens”, “universal saprotrophs” and “endophytes” were 1.1–2.4-fold higher in 1000 µm mesh treatment than in 1 µm mesh ($p\text{-adj} \leq 0.05$ with DESeq2, data not shown), whereas the proportion of “undefined saprotrophs” was 1.3-fold higher in 1µm mesh treatments than in 1000 µm mesh ($p\text{-adj} \leq 0.05$ with DESeq2, data not shown). In addition, the proportion of fungal guild “wood saprotrophs” was 1.5-fold higher in 1000 µm mesh treatments than in 50 µm and 1 µm mesh ($p\text{-adj} \leq 0.05$ with DESeq2, data not shown).

Tables:

Table 1. Richness (observed and estimated OTUs), evenness and diversity indices for a) fungal ITS2 region libraries and b) bacterial 16S rDNA region libraries in the different mesh treatments across the three growing seasons. Average values and standard deviations are calculated with all the replicates (N=15). Statistical significance of the diversity indices was obtained with Kruskal-Wallis test. Levels of statistical significances ($p \leq 0.05$) within each mesh size between growing seasons are marked with letters.

a)

		Sequence count	Observed	Estimated	Subsampled fungal OTUs			Pielou's evenness
					Shannon	InvSimpson	Fisher	
1st growing season	1 μ m	1 119 433	631 \pm 69	707 \pm 75	3.52 \pm 0.92	15.05 \pm 15.99	102.13 \pm 13.17	1.25 \pm 0.31
	50 μ m	1 105 068	625 \pm 69	710 \pm 84	3.57 \pm 0.82	15.25 \pm 13.37	101.05 \pm 13.33	1.28 \pm 0.28
	1000 μ m	1 095 877	626 \pm 93	710 \pm 110	3.41 \pm 0.91	12.76 \pm 11.64	101.36 \pm 17.86	1.21 \pm 0.30
2nd growing season	1 μ m	1 158 280	549 \pm 42	628 \pm 51	3.33 \pm 0.47	8.87 \pm 5.60	86.48 \pm 7.74	1.21 \pm 0.16
	50 μ m	1 194 473	576 \pm 55	667 \pm 64	3.32 \pm 0.72	9.72 \pm 8.35	91.74 \pm 10.29	1.20 \pm 0.25
	1000 μ m	1 294 510	561 \pm 59	649 \pm 68	3.22 \pm 0.73	10.15 \pm 11.47	88.95 \pm 11.03	1.17 \pm 0.25
3rd growing season	1 μ m	1 283 097	525 \pm 51	598 \pm 64	3.09 \pm 0.49	7.12 \pm 3.44	82.17 \pm 9.38	1.13 \pm 0.17
	50 μ m	1 320 903	533 \pm 47	624 \pm 65	3.23 \pm 0.60	9.47 \pm 6.32	83.59 \pm 8.75	1.18 \pm 0.21
	1000 μ m	1 483 150	524 \pm 40	609 \pm 43	3.04 \pm 0.46	7.09 \pm 6.04	81.94 \pm 7.44	1.12 \pm 0.16

b)

		Sequence count	Observed	Estimated	Subsampled bacterial OTUs			Pielou's evenness
					Shannon	InvSimpson	Fisher	
1st growing season	1 μ m	1 605 945	1508 \pm 57	2147 \pm 75	5.78 \pm 0.06	122.05 \pm 7.90	375.74 \pm 18.81	1.82 \pm 0.01
	50 μ m	1 520 772	1490 \pm 64	2071 \pm 133	5.76 \pm 0.09	121.14 \pm 10.33	369.59 \pm 20.90	1.82 \pm 0.02
	1000 μ m	1 555 333	1481 \pm 86	2064 \pm 116	5.76 \pm 0.11	121.03 \pm 10.56	367.03 \pm 28.15	1.82 \pm 0.02
2nd growing season	1 μ m	1 365 140	1303 \pm 204	1824 \pm 266	5.46 \pm 0.28	88.30 \pm 18.33	311.79 \pm 61.32	1.76 \pm 0.05
	50 μ m	1 304 927	1272 \pm 191	1761 \pm 260	5.43 \pm 0.24	84.93 \pm 14.96	301.97 \pm 58.09	1.75 \pm 0.04
	1000 μ m	1 281 568	1342 \pm 132	1869 \pm 210	5.51 \pm 0.18	89.58 \pm 13.68	322.96 \pm 40.84	1.76 \pm 0.04
3rd growing season	1 μ m	879 696	1349 \pm 87	1776 \pm 152	5.55 \pm 0.10	87.15 \pm 6.54	324.49 \pm 27.48	1.77 \pm 0.02
	50 μ m	922 043	1268 \pm 182	1666 \pm 285	5.43 \pm 0.24	82.43 \pm 14.59	300.56 \pm 55.41	1.75 \pm 0.04
	1000 μ m	886 280	1331 \pm 149	1793 \pm 205	5.49 \pm 0.20	84.62 \pm 10.46	319.62 \pm 45.92	1.76 \pm 0.04

Table 2. The total number of OTUs, sequences and relative share of sequences (percentage of total sequence count) of fungal OTUs in different phyla, orders and genera, their relative abundances (percentages of the total sequence count per sample) and the standard deviation in different mesh treatments. The average values are calculated with all the replicates (N=15). The fungal genera and species did not correlate significantly with the environmental variables.

Taxonomy	total %	number of sequences	number of OTUs	1st growing season			2nd growing season			3rd growing season		
				1 μ m	50 μ m	1000 μ m	1 μ m	50 μ m	1000 μ m	1 μ m	50 μ m	1000 μ m
Basidiomycota	62.9	6 950 964	796	53.3 \pm 15.1	50.8 \pm 14.8	56.2 \pm 13.8	63.3 \pm 10.9	62.7 \pm 12.8	66.3 \pm 10.9	68.5 \pm 7.7	64.8 \pm 11.4	68.5 \pm 12.4
Agaricales	5.5	609 096	144	7.2 \pm 13.9	1.5 \pm 1.0	3.7 \pm 6.6	9.1 \pm 16.3	5.2 \pm 9.3	3.3 \pm 5.2	7.5 \pm 14.1	7.3 \pm 9.9	2.7 \pm 3.4
Cortinarius	2.7	298 180	64	0.95 \pm 0.39	0.78 \pm 0.22	0.73 \pm 0.23	7.3 \pm 16.6	3.3 \pm 8.4	1.09 \pm 1.09	5.55 \pm 13.90	3.20 \pm 7.42	1.16 \pm 1.83
Inocybe	1.1	124 832	4	3.80 \pm 13.28	0.00 \pm 0.00	1.06 \pm 4.01	0.40 \pm 1.53	0.10 \pm 0.37	0.38 \pm 1.44	0.25 \pm 0.96	1.72 \pm 6.64	0.77 \pm 2.85
Atheliales	19.1	2 108 101	152	4.35 \pm 5.20	5.85 \pm 7.02	6.87 \pm 7.64	20.3 \pm 16.7	17.9 \pm 19.5	26.8 \pm 20.0	20.4 \pm 16.2	24.4 \pm 17.9	29.2 \pm 23.0
Piloderma	9.9	1 092 768	105	2.23 \pm 4.92	2.83 \pm 4.57	2.36 \pm 4.19	5.7 \pm 7.2	7.8 \pm 10.4	14.8 \pm 16.5	10.3 \pm 11.1	14.7 \pm 19.6	18.2 \pm 21.3
Tylospora	9.2	1 012 782	43	2.11 \pm 2.56	3.02 \pm 5.26	4.51 \pm 4.58	14.6 \pm 14.4	10.0 \pm 14.3	11.9 \pm 16.0	10.1 \pm 12.2	9.77 \pm 8.91	11.0 \pm 10.6
Boletales	2.4	265 572	29	1.05 \pm 0.57	3.23 \pm 5.31	4.04 \pm 6.89	0.97 \pm 0.55	1.27 \pm 1.45	4.75 \pm 7.42	1.12 \pm 1.87	1.05 \pm 1.52	4.62 \pm 9.66
Suillus	1.6	175 044	21	0.13 \pm 0.26	2.27 \pm 5.23	3.17 \pm 6.94	0.25 \pm 0.49	0.58 \pm 1.48	3.06 \pm 6.66	0.56 \pm 1.88	0.49 \pm 1.53	4.17 \pm 9.73
Suillus bovinus	0.8	91 725	2	0.07 \pm 0.20	0.02 \pm 0.06	2.67 \pm 7.00	0.06 \pm 0.15	0.38 \pm 1.47	0.44 \pm 1.19	0.54 \pm 1.89	0.42 \pm 1.53	3.12 \pm 9.71
Suillus tomentosus	0.002	23 406	3	0.002 \pm 0.00	0.009 \pm 0.016	0.31 \pm 0.82	0.07 \pm 0.23	0.05 \pm 0.11	0.99 \pm 2.76	0.00 \pm 0.00	0.01 \pm 0.04	0.30 \pm 1.15
Russulales	21.2	2 338 129	94	29.3 \pm 27.3	26.4 \pm 27.1	31.9 \pm 27.5	17.6 \pm 19.8	16.4 \pm 18.3	11.9 \pm 14.9	26.8 \pm 25.0	17.5 \pm 22.1	20.4 \pm 21.8
Lactarius	14.2	1 572 147	46	24.8 \pm 29.1	23.4 \pm 26.8	28.6 \pm 28.3	8.7 \pm 13.9	7.2 \pm 9.3	5.8 \pm 10.8	15.2 \pm 23.5	9.7 \pm 17.9	10.6 \pm 17.2
Russula	6.9	765 982	48	4.5 \pm 11.8	2.9 \pm 6.9	3.3 \pm 12.3	8.9 \pm 14.1	9.2 \pm 16.3	6.1 \pm 13.0	11.6 \pm 18.7	7.8 \pm 17.5	9.8 \pm 18.6
Russula decolorans	2.3	260 994	3	2.11 \pm 8.14	1.61 \pm 6.18	1.24 \pm 4.78	2.49 \pm 9.61	3.26 \pm 12.47	2.89 \pm 11.15	3.98 \pm 14.98	4.0 \pm 15.4	4.0 \pm 15.3
Trechisporales	3.1	346 768	35	1.67 \pm 2.89	1.54 \pm 4.10	0.57 \pm 1.71	2.37 \pm 8.00	6.08 \pm 21.83	6.22 \pm 20.76	0.51 \pm 1.39	0.19 \pm 0.43	3.80 \pm 14.21
Sistotremastrum	3.0	326 751	11	1.53 \pm 2.89	1.46 \pm 4.06	0.49 \pm 1.70	2.18 \pm 8.01	6.01 \pm 21.85	5.40 \pm 20.85	0.47 \pm 1.39	0.14 \pm 0.43	3.73 \pm 14.22
Ascomycota	28.9	3 193 635	1098	35.7 \pm 11.7	39.2 \pm 12.6	34.5 \pm 10.8	29.3 \pm 9.0	29.4 \pm 10.1	26.2 \pm 8.5	23.5 \pm 5.5	27.5 \pm 9.0	24.0 \pm 8.7
Chaetothyriales	3.9	428 503	123	3.95 \pm 1.67	4.77 \pm 2.68	4.42 \pm 2.25	4.32 \pm 1.57	4.63 \pm 2.10	4.28 \pm 2.09	3.21 \pm 0.90	3.36 \pm 1.16	3.30 \pm 0.81
Helotiales	9.3	1 030 661	245	12.5 \pm 4.3	13.3 \pm 4.4	11.7 \pm 3.2	9.2 \pm 3.8	8.8 \pm 2.7	8.0 \pm 2.1	7.4 \pm 2.0	9.0 \pm 4.2	7.0 \pm 2.1
Leotiomycetes order Incerta	4.3	480 067	168	5.38 \pm 1.76	5.68 \pm 1.71	5.06 \pm 1.82	4.49 \pm 1.51	4.53 \pm 1.54	4.29 \pm 1.41	3.60 \pm 0.85	3.91 \pm 1.32	3.56 \pm 1.10
Oidiodendron	3.2	359 211	108	4.00 \pm 1.25	4.12 \pm 1.24	3.78 \pm 1.34	3.32 \pm 1.19	3.39 \pm 1.23	3.28 \pm 1.19	2.69 \pm 0.64	2.95 \pm 1.01	2.74 \pm 0.91
Oidiodendron pillicola	2.0	223 394	59	2.37 \pm 0.75	2.55 \pm 0.76	2.24 \pm 0.68	2.16 \pm 0.84	2.23 \pm 0.91	1.90 \pm 0.65	1.74 \pm 0.36	1.93 \pm 0.70	1.66 \pm 0.56
Oidiodendron maius	0.4	41 887	13	0.54 \pm 0.25	0.53 \pm 0.25	0.51 \pm 0.27	0.28 \pm 0.15	0.30 \pm 0.21	0.59 \pm 0.53	0.15 \pm 0.09	0.23 \pm 0.22	0.42 \pm 0.41
Mucoromycota	5.4	600 684	219	8.1 \pm 2.2	7.3 \pm 1.5	6.4 \pm 1.8	5.2 \pm 1.6	5.4 \pm 1.5	5.0 \pm 1.3	4.6 \pm 0.8	4.7 \pm 1.6	4.0 \pm 1.4
Mortierellales	2.9	322 917	108	4.42 \pm 1.91	4.09 \pm 1.22	3.63 \pm 1.68	2.60 \pm 1.44	2.90 \pm 1.22	2.77 \pm 1.07	2.39 \pm 0.58	2.46 \pm 1.28	2.15 \pm 1.16
Mortierella	2.7	301 765	99	4.15 \pm 1.84	3.81 \pm 1.18	3.27 \pm 1.37	2.41 \pm 1.42	2.72 \pm 1.20	2.58 \pm 1.06	2.26 \pm 0.57	2.31 \pm 1.28	2.04 \pm 1.16
Mucorales	2.5	274 748	105	3.64 \pm 1.10	3.23 \pm 0.96	2.81 \pm 0.77	2.64 \pm 0.77	2.54 \pm 0.91	2.19 \pm 0.78	2.20 \pm 0.50	2.29 \pm 0.91	1.82 \pm 0.70
Umbelopsis	2.1	232 126	85	2.84 \pm 0.93	2.62 \pm 0.78	2.35 \pm 0.60	2.25 \pm 0.68	2.18 \pm 0.79	1.90 \pm 0.63	1.92 \pm 0.43	2.02 \pm 0.80	1.62 \pm 0.62
Rozellomycota	0.13	14 359	21	0.19 \pm 0.08	0.17 \pm 0.06	0.19 \pm 0.07	0.14 \pm 0.09	0.14 \pm 0.06	0.11 \pm 0.05	0.09 \pm 0.04	0.11 \pm 0.07	0.09 \pm 0.06
Glomeromycota	0.11	11 885	9	0.18 \pm 0.31	0.16 \pm 0.35	0.20 \pm 0.33	0.10 \pm 0.13	0.17 \pm 0.30	0.09 \pm 0.11	0.04 \pm 0.06	0.05 \pm 0.11	0.05 \pm 0.12
Zoopagomycota	0.001	73	2	0.04 \pm 3.60	0.03 \pm 2.56	0.03 \pm 3.03	0.03 \pm 2.62	0.03 \pm 2.50	0.03 \pm 1.91	0.02 \pm 1.21	0.02 \pm 2.62	0.02 \pm 2.20
Chytridiomycota	0.002	229	4	0.004 \pm 0.006	0.007 \pm 0.008	0.005 \pm 0.007	0.002 \pm 0.005	0.001 \pm 0.001	0.005 \pm 0.005	0.002 \pm 0.005	0.001 \pm 0.002	0.001 \pm 0.001
unclassified	2.6	282 892	417	2.5 \pm 0.9	2.3 \pm 0.8	2.5 \pm 2.0	1.9 \pm 0.6	2.0 \pm 0.8	2.3 \pm 1.5	3.3 \pm 3.8	2.8 \pm 1.6	3.4 \pm 3.4

Table 3. The total number of OTUs, sequences and relative share of sequences (percentage of total sequence count) of bacterial OTUs in main phyla, classes, orders and genera, their relative abundances (percentages of the total sequence count per sample) and the standard deviation in different mesh treatments. The average values are calculated with all the replicates (N=15). The statistically significant ($p \leq 0.05$) R-values of Spearman correlations of the individual phyla, class, order and genus with the environmental variables (see Supplementary Table 2) are represented. ns=not statistically significant correlation.

Taxonomy	total %	number of sequences	number of OTUs	1st growing season			2nd growing season			3rd growing season			Spearman correlations		
				1 μ m	50 μ m	1 mm	1 μ m	50 μ m	1 mm	1 μ m	50 μ m	1 mm	pH	moisture	mass loss
Proteobacteria	39.6	4 486 527	2783	38.5 \pm 1.0	39.3 \pm 1.9	38.6 \pm 1.4	40.2 \pm 2.3	40.3 \pm 1.7	40.2 \pm 1.8	40.1 \pm 1.3	40.6 \pm 1.9	40.0 \pm 1.1	ns	ns	ns
Alphaproteobacteria	25.7	2 910 329	716	23.0 \pm 0.9	24.2 \pm 1.7	23.7 \pm 1.1	27.1 \pm 2.7	27.5 \pm 1.8	27.1 \pm 2.1	27.0 \pm 1.3	27.4 \pm 1.4	26.7 \pm 1.2	ns	-0.56	0.60
Caulobacteriales	2.1	243 841	51	2.5 \pm 0.3	2.6 \pm 0.2	2.6 \pm 0.3	1.8 \pm 0.4	2.0 \pm 0.3	2.1 \pm 0.2	1.7 \pm 0.3	1.8 \pm 0.3	1.7 \pm 0.2	ns	0.56	-0.59
Phenylobacterium	1.4	163 364	24	1.6 \pm 0.1	1.8 \pm 0.2	1.7 \pm 0.2	1.3 \pm 0.3	1.4 \pm 0.2	1.4 \pm 0.1	1.1 \pm 0.2	1.2 \pm 0.2	1.1 \pm 0.1	ns	0.52	-0.61
Rhizobiales	15.7	1 753 630	167	14.0 \pm 0.7	14.0 \pm 0.5	13.9 \pm 0.3	15.8 \pm 1.6	16.7 \pm 1.5	16.8 \pm 1.4	16.9 \pm 1.0	16.7 \pm 1.3	16.6 \pm 1.2	ns	-0.60	0.55
Rhizomicrobium	2.1	237 665	37	2.6 \pm 0.3	2.4 \pm 0.2	2.5 \pm 0.3	1.7 \pm 0.3	1.8 \pm 0.3	2.0 \pm 0.4	1.7 \pm 0.3	1.6 \pm 0.3	1.9 \pm 0.3	ns	0.57	-0.52
Variibacter	4.3	487 414	15	3.5 \pm 0.2	3.2 \pm 0.3	3.3 \pm 0.2	4.7 \pm 0.9	4.9 \pm 0.8	4.8 \pm 0.7	5.6 \pm 0.6	5.1 \pm 0.8	4.9 \pm 1.0	ns	ns	0.56
Rhodospirillales	7.2	796 766	198	5.3 \pm 0.3	6.5 \pm 1.7	6.1 \pm 0.9	8.5 \pm 3.6	7.9 \pm 1.3	7.4 \pm 2.0	7.4 \pm 1.1	8.0 \pm 1.8	7.5 \pm 1.4	ns	ns	ns
Acidicaldus	0.9	97 103	8	0.6 \pm 0.1	0.7 \pm 0.1	0.6 \pm 0.1	1.0 \pm 0.2	1.0 \pm 0.1	0.9 \pm 0.1	1.1 \pm 0.1	1.0 \pm 0.1	1.0 \pm 0.2	ns	ns	0.63
Acidocella	1.2	136 844	17	0.8 \pm 0.1	1.4 \pm 1.2	1.0 \pm 0.6	1.6 \pm 2.6	1.3 \pm 0.7	1.1 \pm 1.3	1.0 \pm 0.6	1.4 \pm 1.3	1.3 \pm 1.0	ns	ns	ns
Gammaproteobacteria	7.2	814 282	1090	7.7 \pm 0.6	7.3 \pm 0.6	7.5 \pm 0.5	6.7 \pm 2.0	6.3 \pm 1.0	7.3 \pm 1.7	7.3 \pm 0.6	7.0 \pm 1.2	8.2 \pm 1.2	ns	ns	ns
Deltaproteobacteria	4.5	511 695	751	5.6 \pm 0.3	5.2 \pm 0.6	5.1 \pm 0.6	4.3 \pm 1.2	4.3 \pm 0.8	3.7 \pm 1.0	4.0 \pm 0.5	3.9 \pm 1.0	3.2 \pm 1.1	0.62	0.75	-0.59
Myxococcales	2.7	314 095	251	3.5 \pm 0.3	3.2 \pm 0.5	3.2 \pm 0.6	2.5 \pm 1.0	2.5 \pm 0.8	2.2 \pm 0.9	2.5 \pm 0.5	2.4 \pm 0.9	1.9 \pm 0.9	0.60	0.67	-0.49
Haliangium	0.9	104 757	36	1.3 \pm 0.2	1.1 \pm 0.3	1.1 \pm 0.3	0.9 \pm 0.4	0.8 \pm 0.3	0.8 \pm 0.4	0.7 \pm 0.2	0.7 \pm 0.4	0.6 \pm 0.3	0.68	0.58	-0.50
Sorangium	1.2	130 924	66	1.4 \pm 0.1	1.4 \pm 0.2	1.4 \pm 0.2	1.0 \pm 0.4	1.0 \pm 0.3	0.9 \pm 0.3	1.1 \pm 0.2	1.0 \pm 0.4	0.9 \pm 0.4	ns	0.67	ns
Acidobacteria	26.6	3 013 927	397	24.3 \pm 1.2	24.0 \pm 1.5	23.9 \pm 1.4	28.5 \pm 3.4	28.2 \pm 4.5	28.6 \pm 4.8	28.1 \pm 1.9	27.5 \pm 3.6	29.5 \pm 3.4	-0.48	-0.59	0.44
Acidobacteria	26.6	3 009 871	392	24.3 \pm 1.2	24.0 \pm 1.5	23.9 \pm 1.4	28.5 \pm 3.4	28.1 \pm 4.5	28.5 \pm 4.8	28.0 \pm 1.9	27.4 \pm 3.6	29.4 \pm 3.4	-0.48	-0.58	0.44
Acidobacteriales	15.9	1 778 870	185	14.8 \pm 0.9	15.1 \pm 1.4	14.9 \pm 1.3	16.4 \pm 3.0	16.4 \pm 2.4	16.4 \pm 2.4	15.5 \pm 1.3	15.9 \pm 3.1	17.2 \pm 4.0	-0.50	ns	ns
Acidobacterium	2.7	301 713	28	2.5 \pm 0.2	2.5 \pm 0.3	2.5 \pm 0.2	2.8 \pm 0.7	2.9 \pm 0.6	2.8 \pm 0.6	2.6 \pm 0.3	2.8 \pm 0.5	3.0 \pm 0.9	-0.45	-0.50	ns
Granulicella	5.0	562 965	44	4.7 \pm 0.5	5.3 \pm 1.2	4.9 \pm 1.1	5.1 \pm 2.9	5.0 \pm 1.7	5.0 \pm 1.5	4.4 \pm 1.2	5.2 \pm 2.3	5.6 \pm 3.2	ns	ns	ns
Telmatobacter	1.7	189 802	18	1.6 \pm 0.2	1.6 \pm 0.3	1.6 \pm 0.2	1.6 \pm 0.4	1.6 \pm 0.4	1.6 \pm 0.3	2.0 \pm 0.3	1.8 \pm 0.4	1.9 \pm 0.4	ns	ns	ns
Actinobacteria	16.5	1 872 279	462	17.2 \pm 1.1	17.4 \pm 1.3	17.9 \pm 1.4	16.7 \pm 3.2	16.3 \pm 3.8	16.6 \pm 4.1	14.6 \pm 1.5	15.0 \pm 1.3	14.8 \pm 2.2	ns	ns	ns
Actinobacteria	9.4	1 064 727	207	9.7 \pm 0.8	10.0 \pm 0.8	10.3 \pm 0.9	9.5 \pm 1.5	9.3 \pm 1.5	9.5 \pm 2.0	8.1 \pm 0.9	8.5 \pm 0.9	8.5 \pm 1.1	ns	ns	ns
Acidimicrobia	3.5	393 103	78	3.5 \pm 0.4	3.6 \pm 0.4	3.4 \pm 0.5	3.6 \pm 1.1	3.6 \pm 1.3	3.6 \pm 1.3	3.2 \pm 0.5	3.3 \pm 0.5	3.0 \pm 0.8	ns	ns	ns
Planctomycetes	5.2	583 176	530	5.1 \pm 0.5	4.9 \pm 0.4	5.0 \pm 0.6	5.3 \pm 0.9	5.5 \pm 0.8	5.2 \pm 0.7	5.1 \pm 0.4	5.0 \pm 0.8	4.6 \pm 0.8	ns	ns	ns
Planctomycetacia	3.2	365 273	391	3.1 \pm 0.3	3.0 \pm 0.3	3.1 \pm 0.5	3.4 \pm 0.6	3.6 \pm 0.7	3.4 \pm 0.6	3.0 \pm 0.3	3.2 \pm 0.5	2.7 \pm 0.5	ns	ns	ns
Verrucomicrobia	4.0	448 927	404	4.7 \pm 0.3	4.6 \pm 0.3	4.8 \pm 0.6	3.0 \pm 1.0	3.1 \pm 0.9	3.0 \pm 0.8	4.3 \pm 0.6	4.2 \pm 0.9	3.9 \pm 0.7	ns	0.56	ns
Bacteroidetes	2.9	326 975	237	4.3 \pm 0.6	3.9 \pm 0.5	4.0 \pm 0.5	1.8 \pm 0.8	1.9 \pm 0.9	2.2 \pm 1.0	2.3 \pm 0.3	2.3 \pm 0.7	2.4 \pm 0.6	ns	0.54	-0.50
Sphingobacteria	2.6	310 796	187	4.1 \pm 0.6	3.7 \pm 0.5	3.8 \pm 0.5	1.7 \pm 0.8	1.8 \pm 0.8	2.1 \pm 1.0	2.2 \pm 0.3	2.1 \pm 0.6	2.2 \pm 0.6	ns	0.52	-0.51
Sphingobacteriales	2.6	310 796	187	4.1 \pm 0.6	3.7 \pm 0.5	3.8 \pm 0.5	1.7 \pm 0.8	1.8 \pm 0.8	2.1 \pm 1.0	2.2 \pm 0.3	2.1 \pm 0.6	2.2 \pm 0.6	ns	0.52	-0.51
Mucilaginibacter	0.8	90 982	76	4.1 \pm 0.6	3.7 \pm 0.5	3.8 \pm 0.5	1.7 \pm 0.8	1.8 \pm 0.8	2.1 \pm 1.0	2.2 \pm 0.3	2.1 \pm 0.6	2.2 \pm 0.6	ns	ns	ns
others	5.0	567 978	1 558	5.7 \pm 1.2	5.7 \pm 1.3	5.5 \pm 1.2	4.3 \pm 1.6	4.5 \pm 1.8	4.1 \pm 1.7	5.2 \pm 1.6	5.3 \pm 2.0	4.6 \pm 1.9	nd	nd	nd
unclassified	0.2	21 915	166	0.2 \pm 0.1	0.2 \pm 0.1	0.2 \pm 0.1	0.2 \pm 0.1	0.2 \pm 0.1	0.2 \pm 0.1	0.2 \pm 0.1	0.2 \pm 0.1	0.2 \pm 0.1	na	na	na

